Dynamic structure of methane/n-nonane clusters during nucleation and growth

Stephan Braun and Thomas Kraska

Citation: The Journal of Chemical Physics **136**, 214506 (2012); doi: 10.1063/1.4723868
View online: http://dx.doi.org/10.1063/1.4723868
View Table of Contents: http://scitation.aip.org/content/aip/journal/jcp/136/21?ver=pdfcov
Published by the AIP Publishing

Dynamic structure of methane/n-nonane clusters during nucleation and growth

Stephan Braun and Thomas Kraska[a)]
Institute for Physical Chemistry, University of Cologne, Luxemburger Str. 116, 50939 Köln, Germany

(Received 14 April 2012; accepted 16 May 2012; published online 4 June 2012)

We report results on nucleation, growth, and structure formation of methane/n-nonane clusters in an expanding system investigated by molecular dynamics simulation. From bulk phase equilibria data, it is expected that the concentration of the less volatile substance n-nonane in the clusters is very high. However, analyses of experimental data in the literature suggest somewhat higher methane content at onset of nucleation. Our simulations show that the methane mole fraction is actually very high and increases even further at the beginning of the cluster growth. On the other hand, in this transient state after nucleation the methane mole fraction in the cluster core decreases, leaving a n-nonane rich core, i.e., we observe the phase separation inside the growing cluster. Methane is squeezed out from the core to the surface and then evaporates from the surface shell during expansion of the system. [http://dx.doi.org/10.1063/1.4723868]

I. INTRODUCTION

The understanding of nucleation has gained wide attention in the context of atmospheric aerosol formation. This is, at least, binary nucleation of substances interacting by strong directional forces, namely, hydrogen bonding. Especially the understanding of the properties of the critical cluster for such system is a topical area of research. Binary systems interacting by van der Waals forces can be regarded as reference systems for those with directional forces. In this context, the question is which effects are already present in van der Waals systems?

The idea that binary clusters formed by nucleation in a vapour are not necessarily well mixed was first discussed in the 1980s. That discussion focused on systems containing water, which are relevant for atmospheric processes and had to rely on analysis of experimental data with theories. In this context, nucleation has been investigated with nucleation theories especially for mixtures of water with alkanols. The extensions of classical nucleation theory to binary systems[1,2] have not been able to model the critical supersaturation of all these water-alkanol systems quantitatively, especially not the water-ethanol system. Flageollet-Daniel *et al.*[3] have proposed an explanation assuming a surface enrichment of one of the two compounds. This means that critical clusters exhibit demixing between the cluster core and the surface regions. In order to lower the surface energy and hence the total energy of the cluster, they expected the substance with the lower surface tension to be enriched in the surface. With this *ad hoc* model, they were able to describe the critical supersaturation of the alkanol-water system up to high water activities. That work can be regarded as an indirect hint for surface enrichment or even a core-shell structure of critical clusters in water-alkanol systems. Experimentally such structure has been observed only recently by Wyslouzil *et al.*[4] for a water-butanol system.

Wilemski[5] proposed a model that distinguishes between bulk and surface molecules in a cluster. Implementing the Gibbs adsorption isotherm leads to a theory that improves the predictions of the classical nucleation theory. Rasmussen[6] argues that the nucleation process is so fast that the critical cluster cannot relax to a metastable equilibrium with the surrounding vapour phase. The diffusion of molecules in the cluster is too slow for a complete phase separation. Hence, not the equilibrium surface tension but a transient surface tension of the critical cluster is relevant for nucleation theory. He proposed to implement a dynamic surface tension in nucleation theory, which turned out to be suitable describing the nucleation of water-alkanol systems that were otherwise impossible to model.

While there are several theoretical considerations and recent experimental results on the structure of water-alkanol clusters little has been done on binary van der Waals systems. Van der Waals systems are expected to exhibit the underlying binary cluster structure of more complex systems and therefore can be regarded as reference systems. To the best of our knowledge, there are no experimental data on the structure of nucleating binary van der Waals clusters. However, there are theoretical investigations using thermodynamic density functional theory (DFT): Zeng and Oxtoby[7] analysed critical clusters of argon-krypton mixtures modelled by the Lennard-Jones potential. Although this is a rather ideal mixture they found that the critical nucleus exhibits a density profile indicating a slight enrichment of argon in the interface. This is qualitatively in agreement with the experimental observation of the structure of water-alkanol clusters in the sense that the substance with the lower surface tension is enriched in the cluster surface. The introduction of a parameter mimicking the less ideal alkanol-water mixtures has led to an amplification of the surface enrichment.[8] Different kind of critical nuclei have been found in non-ideal Lennard-Jones mixtures

a)E-mail: t.kraska@uni-koeln.de.

with partial immiscibility.[9] The existence of different critical nuclei has also been determined in DFT calculations by Li and Wilemski.[10] Depending on the degree of metastability they found either well-mixed clusters or core-shell structures.

Concerning the binary system investigated here there exist experimental results for the nucleation rates as well as their theoretical analysis. Looijmans *et al.*[11] analysed binary nucleation rate data combining classical nucleation theory with the Redlich-Kwong equation of state describing the real gas behaviour. They obtained a critical methane mole fraction of about 0.1 and concluded that methane cannot be regarded as an inert gas; it rather contributes to a binary nucleation process. Furthermore, Looijmans *et al.*[12] have measured the binary nucleation rates for the system methane/n-nonane and analysed them with the nucleation theorem. They have observed that the methane mole fraction of the critical cluster is as high as 0.77 at 40 bar and decreases to about 0.45 at 10 bar. More recently, Kalikmanov and Labetski[13] have presented a model independent estimation of the critical cluster content of methane. They have found that methane is not involved in the nucleation process at 1 bar, but with raising pressure it becomes involved leading to a high methane mole fraction in the cluster.

Here, we pick up on these theoretical estimations and perform MD simulation to understand the dynamic binary cluster structure. We present MD simulation results on vapour-liquid nucleation of the binary system methane/n-nonane in an expanding system.

II. METHOD

The simulation system is set up by filling a box with 10^5 methane molecules followed by an equilibration run. Then the n-nonane molecules are filled at random in the box. Overlapping methane molecules are removed from the box. This results in roughly 95 000 remaining methane molecules if 343 n-nonane molecules are added. Then this system is equilibrated again. The expansion of the system is represented by a stepwise enlargement of the simulation box. The system is prepared in the initial state at high pressure and high temperature with a *NVT* equilibration run followed by a short *NVE* equilibration run, to exclude possible effects of the thermostat. The box is then expanded stepwise by 0.1 nm in all three dimensions. At each step, a *NVE* equilibration run of 3.5 ps is performed. This constant energy simulation allows the system to expand within the new enlarged simulation box. The method has been developed for modelling the rapid expansion of a supercritical solution process for pharmaceutical particle formation.[14,15] It has been proven to follow the path of an adiabatic expansion for carbon dioxide[14] which we confirmed here for methane comparing simulation results with an accurate reference equation of state.[16] Also, it is important to analyze the influence of the system size because nucleation is a process related to fluctuations which are known to be finite size dependent. Based on earlier investigation of the simulation method,[14] we do not expect an effect for our relatively large system sizes.

The time scales of an expansion in a nozzle and in simulations differ. The limit of an infinitely fast expansion, i.e., in one step only, would correspond to a quench in a single simulation step. Simulation results obtained in such quench simulations have been compared to experimental data by comparing to classical nucleation theory. The agreement between experimental data and simulation data compared in this manner is generally good.[17,18] It follows that the critical supersaturation is reached faster in the expansion simulation than in the experiment, which however does not affect the nucleation process.

TABLE I. Lennard-Jones parameters for the TraPPE model.

Site	ε/k_B (K)	σ (Å)
CH_4	148	3.73
CH_3	98	3.75
CH_2	46	3.95

For the modelling of the molecular interaction, we use the Transferable Potential for Phase Equilibria (TraPPE) force field for both n-nonane and methane.[19] This is an united atom model characterizing n-nonane via nine Lennard-Jones sites each representing a CH_2 or CH_3 group. Methane is described via a single Lennard-Jones site. The corresponding Lennard-Jones parameters are given in Table I. The bond length between the sites is fixed at 1.54 Å, while the bond angle bending is governed by a harmonic potential where the equilibrium angle is set to 114°. The motion of the dihedral angles is described by an united atom torsion potential. This force field has been developed for the accurate simulation of phase equilibria data.

During the expansion the system moves down from high pressure into the co-existence region and eventually phase separation starts by nucleation. We analyse binary clusters taken from these simulations with respect to their composition and structure during the nucleation and growth process. For the detection of the clusters, we use the Stillinger distance[20] criterion combined with a life time criterion.[14] We regard two molecules as connected, if their distance is smaller than the Stillinger distance (1.5σ) over a period of 2 ps. This time period is larger than that of the collision of two molecules eliminating short-living molecule collisions from the cluster detection. The system size and hence the expansion simulations do not affect the cluster detection since the latter depends only on the residence time of a molecule site in the Stillinger sphere.

The system methane/n-nonane exhibits a large vapour-liquid miscibility gap over a wide temperature and pressure range. As visible in Fig. 1, the methane mole fraction in the vapour phase is close to unity (0.9999) while the liquid phase methane mole fraction varies in a range from roughly 0.05 to 0.45 at given conditions. We have set up the initial system in order to represent approximately the composition of a natural gas system, i.e., a system with high methane mole fraction. Using 343 n-nonane molecules and 94 450 methane molecules, the resulting methane mole fraction is 0.9964. The expansion starts at high supercritical density of $\rho(CH_4) = 25.9$ mol/dm^3, 300 K, and high supercritical pressure. It then penetrates the two-phase region of the phase diagram as indicated by points in Fig. 1. During the expansion the temperature decreases, moving the liquid binodal curve to a

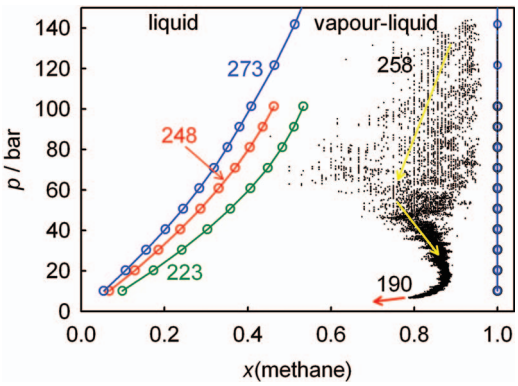

FIG. 1. Bulk phase diagram (interpolated open circles) of the methane/n-nonane system for three different temperatures.[27] The points are the simulation data for the system pressure and the *overall* mole fraction of the largest cluster for an exemplary simulation run. The numbers are temperatures in Kelvin. The path of the largest cluster during expansion is indicated by arrows. In addition, the temperature range of the plotted simulation data is indicated.

slightly higher methane mole faction. The actual conditions of the largest cluster at the onset of nucleation are marked by points in Fig. 1. In the depicted pressure range, the temperature decreases from 258 K to 190 K.

III. RESULTS

We have analysed different systems with approximately 10^5 methane molecules and 125–343 n-nonane molecules, with varying initial conditions in density ranging from 13.3 to 25.9 mol/dm^3 and temperature ranging from 240 to 320 K. In order to study the growth, we focus on the largest cluster in each simulation system. The results for one exemplary simulation run with 343 n-nonane molecules and 94 450 methane molecules are shown in Fig. 1–3. The expansion of this specific system starts at a supercritical density $\rho(CH_4)$ = 25.9 mol/dm^3, 300 K, and supercritical pressure.

A. Overall cluster growth

The growth of the largest cluster is represented in Fig. 2, where the numbers of molecules in the cluster, respectively, the mole fraction is plotted versus the simulation time. The simulation can be divided into 3 domains. In the first 0.3 ns, no cluster formation is taking place. In the second period from 0.3 to 1.2 ns, the cluster starts to grow to a size of about 100 n-nonane molecules. Finally, evaporation phase starts at 1.2 ns. At the beginning, there is no cluster formation besides some density fluctuations. At about 0.3 ns, a cluster forms which then continuous to grow. At the same time methane molecules are attached at the cluster as depicted in Fig. 2(b). This leads to a relatively high methane mole fraction of the forming cluster in the order of 0.8 (Fig. 2(c)).

B. Cluster mole fraction

One can recognize three domains in the development of the cluster mole fraction. First, the methane mole fraction decreases which is caused by dominant n-nonane nucleation.

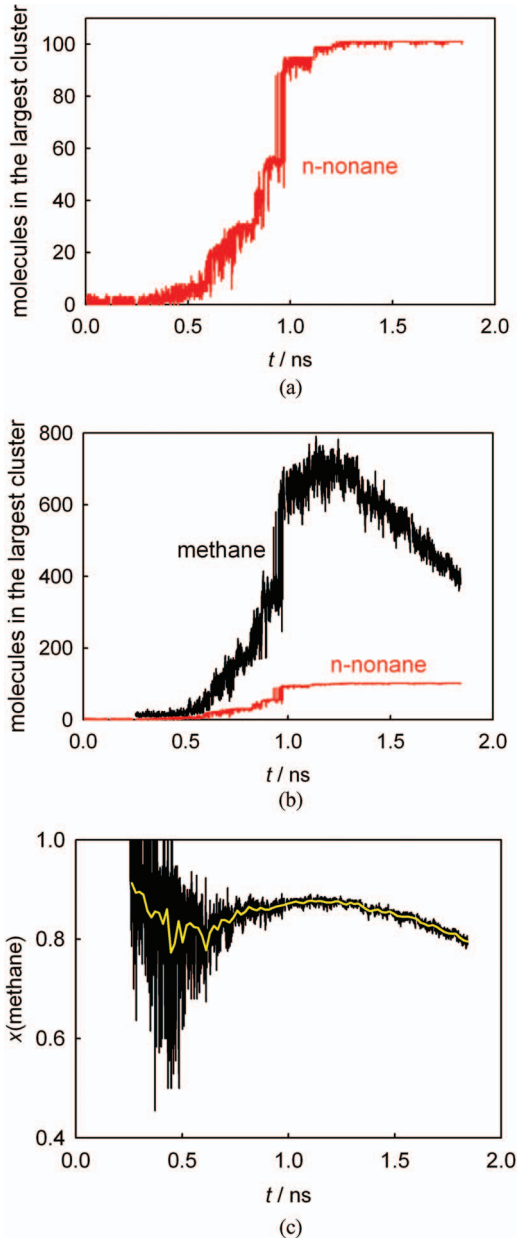

FIG. 2. (a) Number of n-nonane molecules in the largest cluster. (b) Number of methane and n-nonane molecules in the largest cluster. (c) Methane mole fraction of the largest cluster.

Then the methane mole fraction continuously increases. This is related to the condensation of methane on the cluster surface. We have checked that at given conditions the expansion of pure methane does not lead to methane condensation. Hence, the methane condensation is a sole effect of the binary nucleation caused by the formation of a binary cluster followed by condensation of methane on its surface. At about 1.2 ns the largest cluster is composed of 100 n-nonane molecules. In this specific simulation, the cluster does not gain further n-nonane it rather remains constant. The methane mole fraction reaches a maximum. Beyond that maximum the effect of the evaporation of methane from the surface caused by the enlargement of the simulation box leads to a decrease of the methane mole fraction. The larger the volume of the system, the higher the number of molecules in the

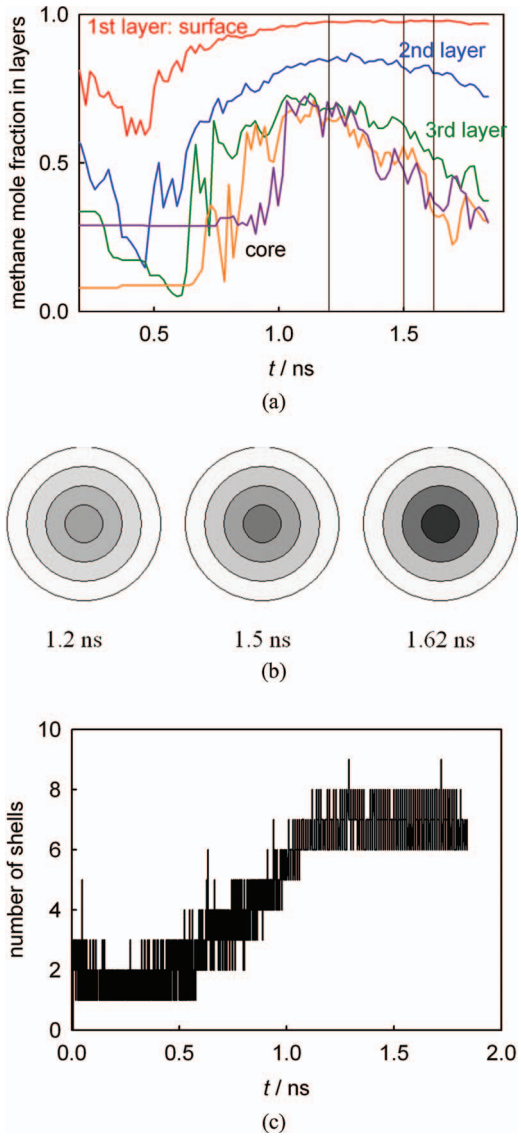

FIG. 3. (a) Methane mole fraction of the different cluster shells from the core to the surface. The vertical lines correspond to the shell diagrams in (b). (b) Schematic cluster structure at different time steps. The shading is calculated from the shell mole fraction. The darker the shell is the higher is the mole fraction of n-nonane. (c) Number of shells of the cluster.

vapour phase. This evaporation of surface methane is not expected to this extent in quench simulations, which do not involve an expansion. However, the evaporation does not take place during nucleation. Hence, with respect to the nucleation process we do not expect any difference in an adiabatically expanding and an isochoric system. Summarizing these results, it seems clear that the methane mole fraction of the cluster surface is very high at the onset of nucleation, i.e., for the critical cluster and also for larger clusters. Since the surface contribution is dominant in small clusters also the overall methane mole fraction of the cluster is higher than the equilibrium mole fraction of the liquid phase. A consequence for the modelling of binary nucleation by theories is that the equilibrium mole fraction of the saturated liquid phase cannot reliably be used for the modelling of the critical cluster. The difference in mole fraction is quite large and hence also other related properties, such as the cluster density and surface tension, are therefore different to their values in the saturated liquid phase. These results are in agreement with the analysis of experimental data using the classical nucleation theory[12] and more general considerations.[13] Actually the simulations here suggest even higher methane content in the critical cluster than expected in earlier theoretical analyses.

C. Cluster structure

It is especially of interest to get an insight into the cluster structure. Here, we have analysed the structure by calculating the number of molecules and hence the mole fraction in each shell of the cluster. For the detection of the cluster surface, we have employed the so-called cone algorithm[21] that we have applied repeatedly after removing the outer shell of the cluster until the core is reached. The resulting mole fractions of the shells are plotted in Fig. 3(a) versus the simulation time. They show different behaviour in the cluster interface and its core. The course of the mole fraction in the surface resembles that of the overall cluster mole fraction. The methane mole fraction in the core however behaves differently. It starts at very low values indicating that it consists of almost pure n-nonane. Later it increases due to the methane condensation. The fact that the core mole fraction changes indicates that the cluster is dynamic, i.e., methane molecules reach the core. Methane is apparently dominant in the surface but not exclusively located there. This trend changes at about 1.2 ns, when the cluster size has reached its maximum and evaporation sets in. We observe a lowering of the methane mole fraction in the core. At the same time (Fig. 2(c)) the overall mole fraction of the cluster decreases while the surface mole fraction is almost constant. This can only be explained by a phase separation taking place in the cluster becoming visible after 1.2 ns. Methane molecules are squeezed out from the core towards the surface by the formation of a n-nonane rich liquid core. At the surface they evaporate which is caused by the expansion of the simulation box as discussed above. Hence, the surface mole fraction remains roughly constant in a steady state situation. One can also recognize in Fig. 3(a) that the cluster core mole fraction reaches values below 0.4 which one would approximately expect from the equilibrium phase diagram of the bulk phases (Fig. 1). Hence, the saturated liquid phase mole fraction and therefore also other properties are apparently similar to those in the cluster core but not to that of the complete cluster or its surface. Figure 3(b) illustrates schematically the inner cluster shells during the demixing. The gray-scale is proportional to the mole fraction of n-nonane: the darker the shell, the higher the n-nonane content. In order to exclude a possible influence of the evaporation on the counting of the shell number, we have plotted in Fig. 3(c) the number of shells as function of the simulation time. In the period of phase separation, the number of shells fluctuates around 7 due to fluctuations of the cluster shape and molecule movement, but it does not shrink despite the fact that some methane molecules evaporate (Fig. 2(b)). This shows that the phase separation is not an effect of a possible vanishing of outer shells but rather a real demixing in the cluster.

It should be noted that the cluster mole fraction plotted in Fig. 1 is the overall mole fraction of the cluster, i.e., an average over core and shell. The core mole fraction is actually not too different from liquid bulk phase mole fraction, but the overall cluster mole fraction is different. In the context of nucleation, the overall mole fraction and the structure of the critical cluster is relevant. The phase separation accelerates later after the cluster has passed its critical size.

IV. CONCLUSIONS

What are the consequences of the observation of demixing in the growing cluster in binary nucleation leading to a dynamic core-shell structure? It appears to confirm the theoretical *ad hoc* considerations of Flageollet-Daniel *et al.*[3] and Wilemski[5] as well as DFT calculations of clusters in metastable equilibrium with the surrounding vapour phase.[7–9] This observation can be understood by the presence of a large surface-bulk ratio and hence a large contribution of the surface energy to the total energy of the system. It is known that due to that contribution the phase diagram of a small cluster differs from that of the bulk phase.[22–24] In case of a pure system, the melting point decreases with decreasing cluster size while the vapour pressure rises. Consequently, the binary phase behaviour is also expected to be different to that of the bulk. The driving force of the phase separation is the instability of a homogenous phase as represented by the phase diagram. There are of course qualitative differences between the bulk phase diagram and the small system (cluster) phase diagram, but both lead to a phase separation.

A consequence is that modelling binary nucleation requires a suitable model for the surface enrichment and the phase separation in the cluster. Such theory should treat the cluster core differently to its surface as, for example, mean field kinetic nucleation theory does.[25] Though the time scale of the simulation is much shorter than that of the corresponding experiments, we expect that also in experiments the critical cluster at the very beginning will unlikely reach its most stable structure or rather metastable equilibrium with the vapour phase. Especially the critical cluster is continuously gaining and loosing molecules. Therefore, it is dynamically changing its structure. Once a cluster has time to rest, i.e., it is not growing for a certain period of time, it starts to separate into the two phases. This is the case here after 1.2 ns when this cluster has reached its final number of n-nonane molecules (Fig. 2(a)). Furthermore, the question arises whether there are differences in the nucleation in either an expanding system or a quenched system. Since the evaporation of methane from the cluster surface takes place only after a certain time when the cluster has time to settle, it does not influence the critical cluster at the onset of nucleation. Therefore, we do not expect an effect of the path towards the supersaturated state on the nucleation behaviour, but it will affect the further growth of the clusters.

Finally, the implication of the observed behaviour is of interest for applications. Separation processes based on nucleation of a heavy compound will have a comparably low efficiency due to the observed effect of a high mole fraction of the low volatile substance in the binary clusters. The other way around it means that even in systems interacting by van der Waals forces traces of heavy compounds can induce nucleation of a vapour at conditions where it otherwise would virtually never nucleate. We would expect that this effect is enhanced in strongly interacting, hydrogen bonding systems. But apparently this effect requires high pressure to see it in van der Waals systems because at ambient pressure the influence of the low volatile component methane on the nucleation is negligible.[13] The pressure effect appears to be comparable to that observed in phase equilibrium investigations, namely, that high pressure and strong interactions have a similar effect. As shown by Schneider,[26] adding strongly interacting ions to aqueous systems at ambient pressure results in very similar phase behaviour as obtained by increasing the pressure. In the context of nucleation similar trends can be expected. The observed effect of van der Waals systems at high pressure is expected to correspond to similar effects of hydrogen bonding systems at ambient pressure.

ACKNOWLEDGMENTS

The authors gratefully acknowledge the support by Twister B.V. and many interesting and helpful discussions with Dr. Vitlaly Kalikmanov and Dr. Judith Wölk.

[1] H. Reiss, J. Chem. Phys. **18**, 840 (1950).
[2] D. Stauffer, J. Aerosol Sci. **7**, 319 (1976).
[3] C. Flageollet-Daniel, J. P. Garnier, and P. Mirabel, J. Chem. Phys. **78**, 2600 (1983).
[4] B. E. Wyslouzil, G. Wilemski, R. Strey, C. H. Heath, and U. Dieregsweiler, Phys. Chem. Chem. Phys. **8**, 54 (2006).
[5] G. Wilemski, J. Chem. Phys. **80**, 170 (1984).
[6] D. H. Rasmussen, J. Chem. Phys. **85**, 2272 (1986).
[7] X. C. Zeng and D. W. Oxtoby, J. Chem. Phys. **95**, 5940 (1991).
[8] A. Laaksonen and D. W. Oxtoby, J. Chem. Phys. **102**, 5803 (1995).
[9] V. Talanquer and D. W. Oxtoby, J. Chem. Phys. **104**, 1993 (1996).
[10] J.-S. Li and G. Wilemski, Phys. Chem. Chem. Phys. **8**, 1266 (2006).
[11] K. N. H. Looijmans, C. C. M. Luijten, G. C. J. Hofmans, and M. E. H. van Dongen, J. Chem. Phys. **102**, 4531 (1995).
[12] K. N. H. Looijmans, C. C. M. Luijten, and M. E. H. van Dongen, J. Chem. Phys. **103**, 1714 (1995).
[13] V. I. Kalikmanov and G. Labetski, Phys. Rev. Lett. **98**, 085701 (2007).
[14] F. Römer and T. Kraska, J. Phys. Chem. C **113**, 19028 (2009).
[15] F. Römer and T. Kraska, J. Supercrit. Fluids **55**, 769 (2010).
[16] U. Setzmann and W. Wagner, J. Phys. Chem. Ref. Data **20**, 1061 (1991).
[17] V. I. Kalikmanov, J. Wölk, and T. Kraska, J. Chem. Phys. **128**, 124506 (2008).
[18] F. Römer and T. Kraska, J. Chem. Phys. **127**, 234509 (2007).
[19] M. G. Martin and J. I. Siepmann, J. Phys. Chem. B **102**, 2569 (1998).
[20] F. H. Stillinger, J. Chem. Phys. **38**, 1486 (1963).
[21] Y. Wang, S. Teitel, and C. Dellago, J. Chem. Phys. **122**, 214722 (2005).
[22] M. Wautelet, J. P. Dauchot, and M. Hecq, Nanotechnology **11**, 6 (2000).
[23] A. S. Shiriayan and M. Wautelet, Nanotechnology **14**, 1720 (2004).
[24] J. Weissmüller, P. Bunzel, and G. Wilde, Scr. Mater. **51**, 813 (2004).
[25] V. I. Kalikmanov, Phys. Rev. E **81**, 050601(R) (2010).
[26] G. M. Schneider, Phys. Chem. Chem. Phys. **4**, 845 (2002).
[27] L. M. Shipman and J. P. Kohn, J. Chem. Eng. Data **11**, 176 (1966).